

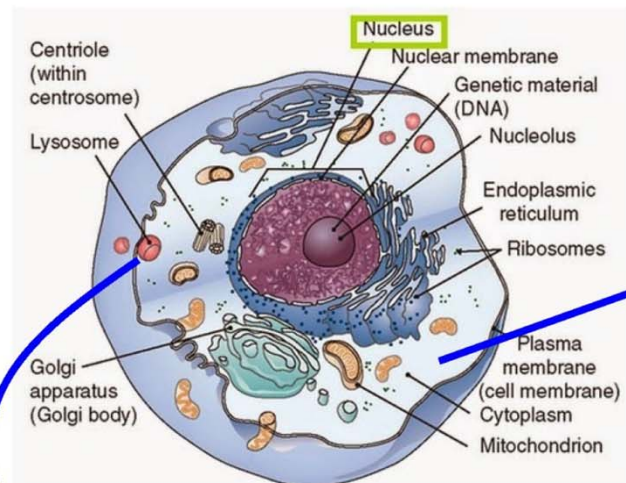
Комп'ютерне моделювання задач прикладної математики

Узагальнення задач броунівського руху.

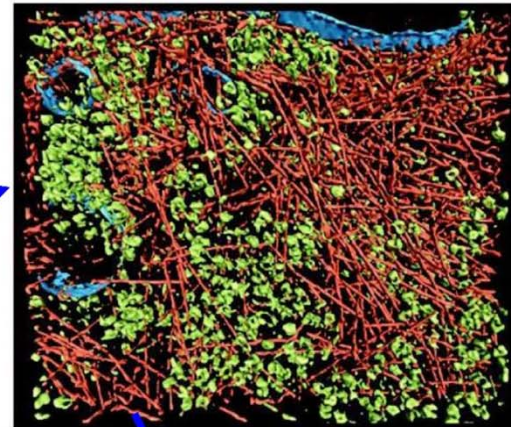
Лекція 6

Inside a Living Cell

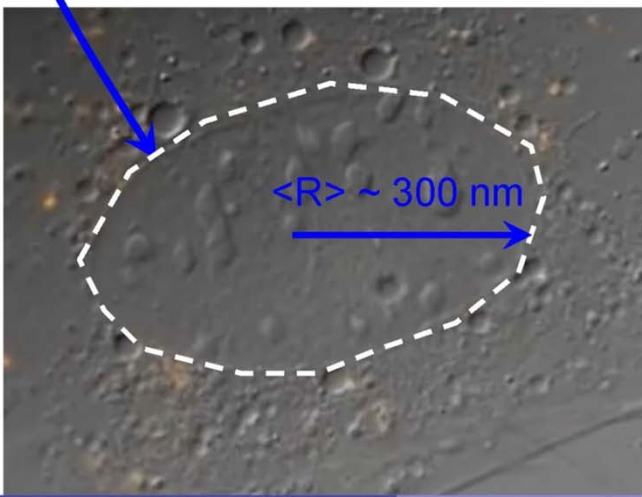
Living Cell



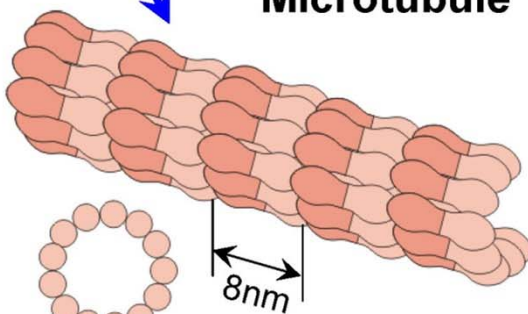
Cytoskeleton



Endosome



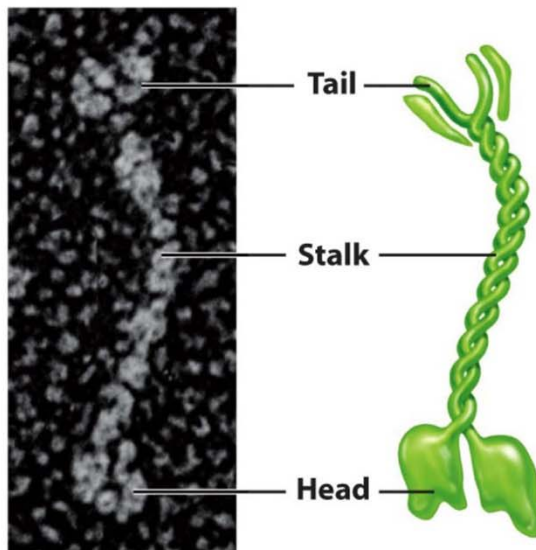
Microtubule



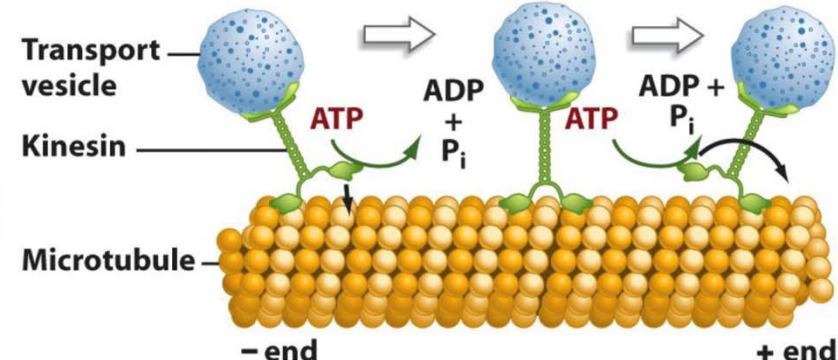
Construction of Microtubules
from α & β Tubulins

Molecular motor

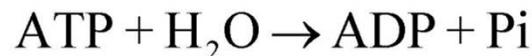
Structure of kinesin



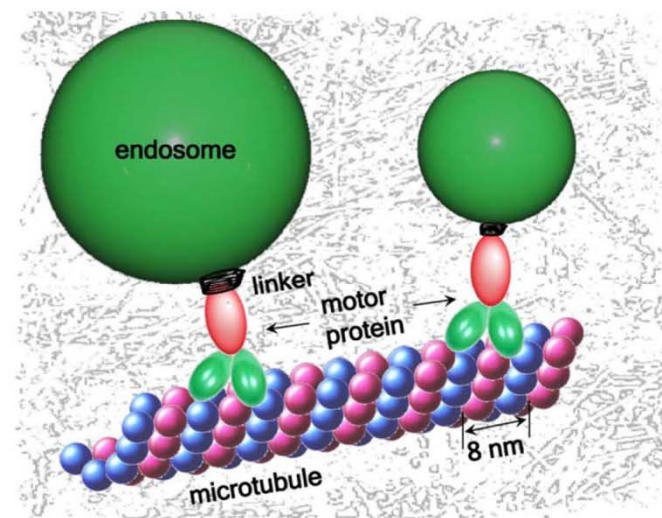
Kinesin “walks” along a microtubule track.



Amount of energy
released from hydrolysis of ATP

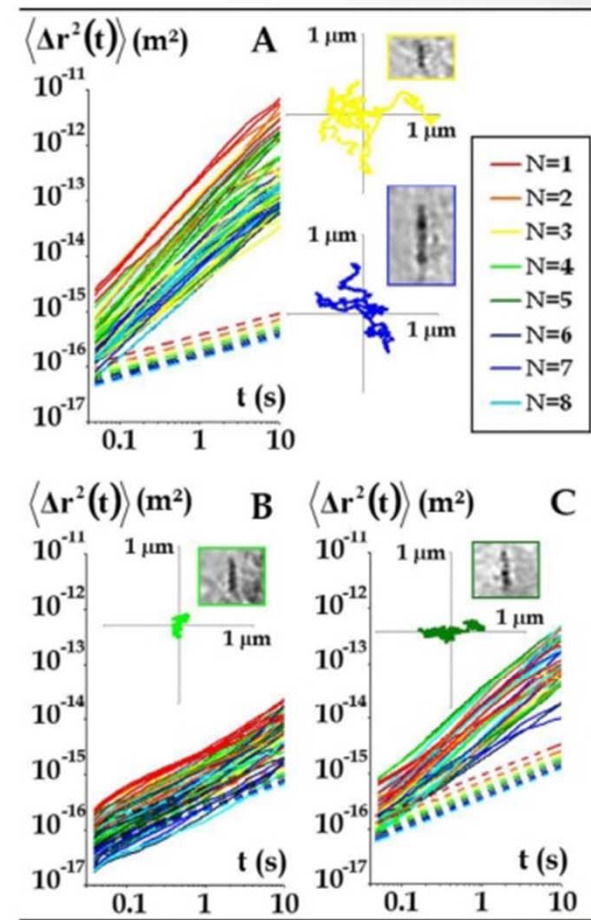
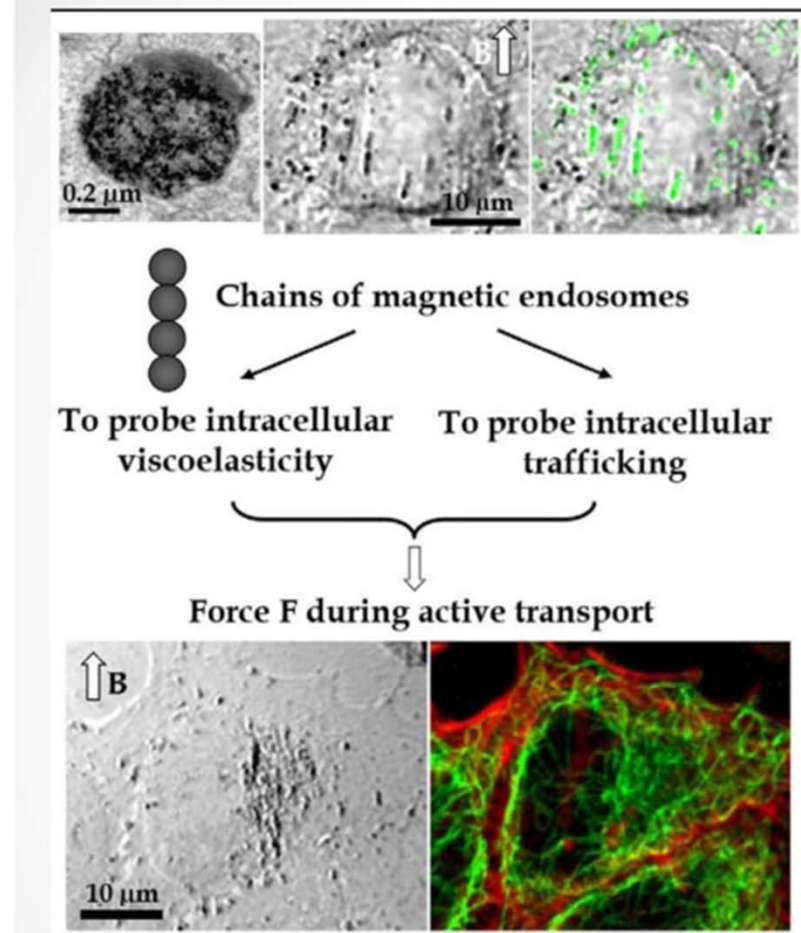


$$\Delta G = -30.5 \text{ kJ/mol}$$



Experimental observations

From: Robert *et al.*, PLoS ONE 5, e10046 (2010)



“Sub diffusion has been proposed as a measure of macromolecular crowding in the cytoplasm.”

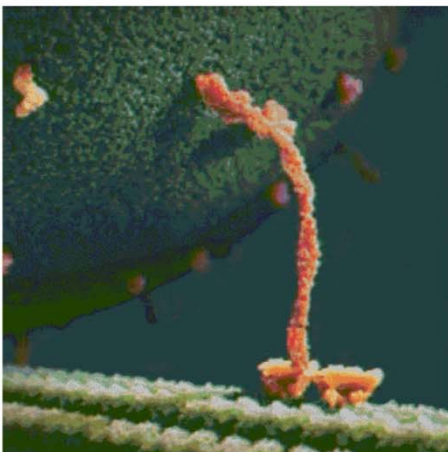


- “Anomalous Subdiffusion Is a Measure for Cytoplasmic Crowding in Living Cells.”

M.Weiss et al. Biophysical Journal 87, 3518 (2004)

- Diffusion of mRNAs and ribosomes in the cytoplasm of living cells
I.Golding and E.C.Cox, Phys. Rev. Lett. 96, 098102 (2006)
- Behavior of large proteins
I.M.Tolic-Norrelykke, et al., Phys. Rev. Lett. 93, 078102 (2004)
- Intrinsic conformational dynamics of the protein macromolecules
H.Yang et al., Science 302, 262 (2003)
R.Granek and J.Klafter, Phys. Rev. Lett. 95, 098106 (2005)
W.Min et al., Phys. Rev. Lett. 94, 198302 (2005)

The problem SetUp



The main question is

How molecular motors work in the crowded environment of living cells?

Tasks

- To construct an adequate model for cargo transport by molecular motors in crowded environment.
- To study properties of anomalous transport.
- To define the thermodynamic efficiency of molecular motor.
- To discuss cargo transport delivery efficiency.

Langevin approach

Normal diffusion case

The original Langevin equation^a describing Brownian motion



$$m \frac{d^2x}{dt^2} = -\gamma \frac{dx}{dt} + f(x) + \xi(t).$$

Term $\xi(t)$ is a Gaussian white noise with

$$\langle \xi_i(t) \xi_j(t') \rangle = 2\gamma k_B T \delta(t - t')$$

according to fluctuation-dissipation relation^b.

^aP.Langevin. “On the Theory of Brownian Motion”. C.R.Acad.Sci. (Paris) 146, 530 (1908)

^bH.Nyquist. Physical Review 32, 110 (1928)

Viscoelastic subdiffusion

Generalized Langevin Equation approach for a Brownian particle:

$$m\ddot{x} + \int_0^t \eta(t-t')\dot{x}(t')dt' + \frac{\partial V(x,t)}{\partial x} = \xi(t). \quad (1)$$

$$V(x,t) = U(x) - Ax \cos(\Omega t) + f_0 x$$

Viscoelastic forces [I.Goychuk, Phys.Rev.E 80, 046125 (2009)]

$$F_{v-el}(t) = - \int_0^t \eta(t-t')\dot{x}(t')dt'. \quad (2)$$

Fluctuation-dissipation relation:

$$\langle \xi(t')\xi(t) \rangle = k_B T \eta(|t-t'|). \quad (3)$$

Memory kernel & force:

- Memoryless linear frictional kernel: $\eta(t) = 2\eta\delta(t) \Rightarrow$
Purely viscous Stokes friction force $F_v = -\eta\dot{x};$
- Constant memory $\eta(t) \equiv \eta = \text{const} \Rightarrow$
Quasielastic force $F_{el}(t) = -\eta [x(t) - x(0)].$

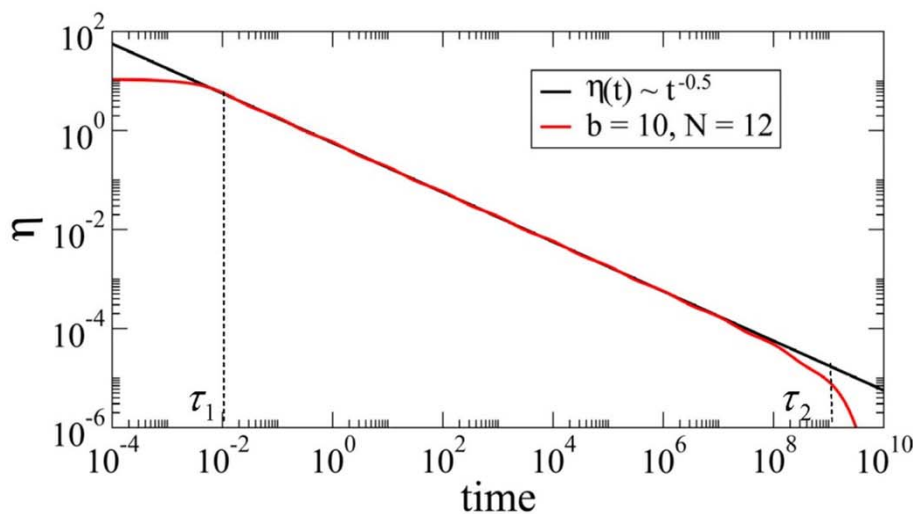
Viscoelastic subdiffusion

A model of viscoelasticity [A.Gemant, Phys. 7, 311 (1936)]

$$\eta(t) = \eta_\alpha t^{-\alpha} / \Gamma(1 - \alpha), \quad \alpha \in (0, 1) \quad (4)$$

Expansion into a sum of exponentials [I.Goychuk, Phys.Rev.E 80, 046125 (2009)]

$$\eta(t) = \sum_{i=1}^N k_i e^{-v_i t}, \quad k_i = \frac{C_\alpha(b) \eta_\alpha}{\Gamma(1 - \alpha)} v_i^\alpha, \quad v_i = \frac{v_0}{b^{i-1}} \quad (5)$$



$$\tau_1 = v_0^{-1}$$

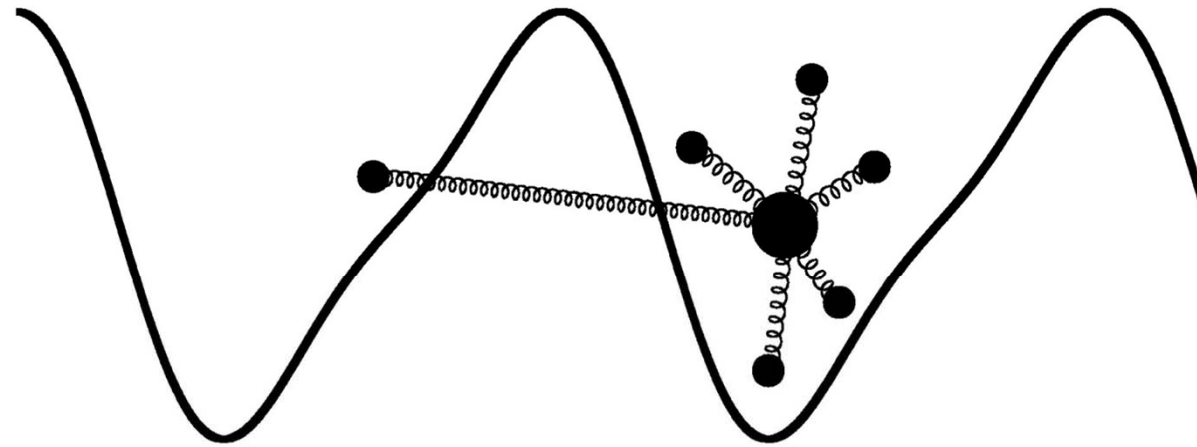
$$\tau_2 = \tau_1 b^{N-1}$$

A model of viscoelasticity [A.Gemant, Phys. 7, 311 (1936)]

$$\eta(t) = \eta_\alpha t^{-\alpha} / \Gamma(1 - \alpha), \quad \alpha \in (0, 1) \quad (6)$$

Expansion into a sum of exponentials [I.Goychuk, Phys.Rev.E 80, 046125 (2009)]

$$\eta(t) = \sum_{i=1}^N k_i e^{-v_i t}, \quad k_i = \frac{C_\alpha(b) \eta_\alpha}{\Gamma(1 - \alpha)} v_i^\alpha, \quad v_i = \frac{v_0}{b^{i-1}} \quad (7)$$



Calculation features

Mean quantities:

At $t \rightarrow \infty$: $\langle x(t) \rangle \propto t^\alpha$, $\langle \delta x^2(t) \rangle \sim 2Tt^\alpha / \Gamma(1 + \alpha)$

Ensemble averaging:

- Number of Brownian particles $M = 10^4$
- Subvelocity $v_\alpha = \Gamma(1 + \alpha) \lim_{t \rightarrow \infty} \frac{\langle x(t) \rangle}{t^\alpha}$
- Dispersion (variance) $\langle \delta x^2(t) \rangle = \langle x^2(t) \rangle - \langle x(t) \rangle^2$



Single trajectory averaging:

- Subvelocity $v_\alpha = \lim_{t \rightarrow \infty} \Gamma(1 + \alpha) x(t) / t^\alpha$
- Dispersion (variance) $\langle \delta x^2(t) \rangle = \frac{1}{T-t'} \int_0^{T-t'} [x(t+t') - x(t')]^2 dt'$

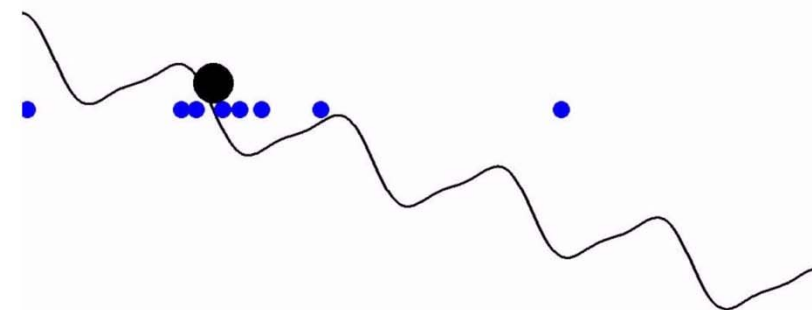
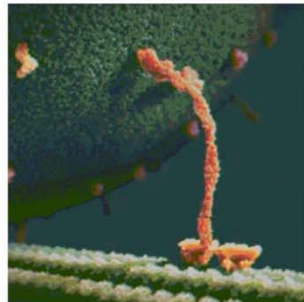
Subdiffusion coefficient: $D_\alpha = \frac{1}{2} \Gamma(1 + \alpha) \lim_{t \rightarrow \infty} \frac{\langle \delta x^2(t) \rangle}{t^\alpha}$, $D_\alpha \simeq T$.

Earlier models: fluctuating tilt subdiffusive ratchets

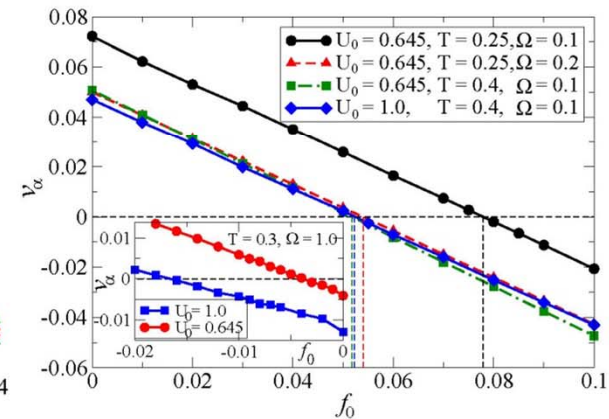
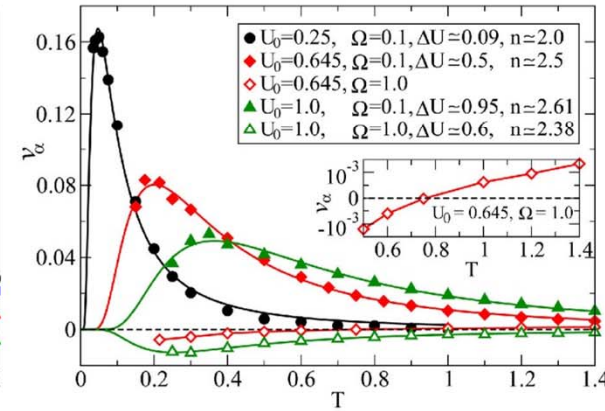
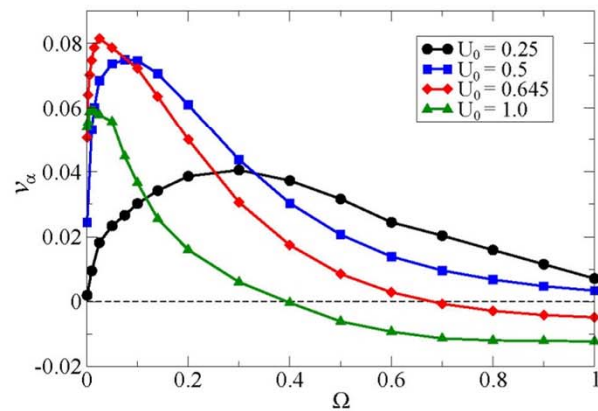
[I.Goychuk, V.Kharchenko

PRE, V.85, 051131 (2012); PRE, V.87, 052119 (2013); MMNP, V.8, 144 (2013)]

Interpretation



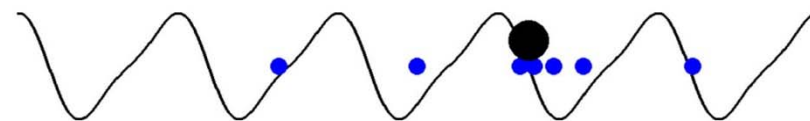
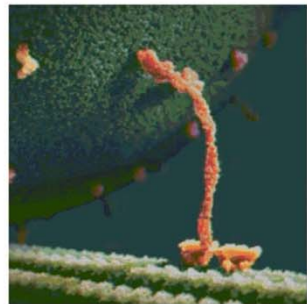
Transport optimization and useful work



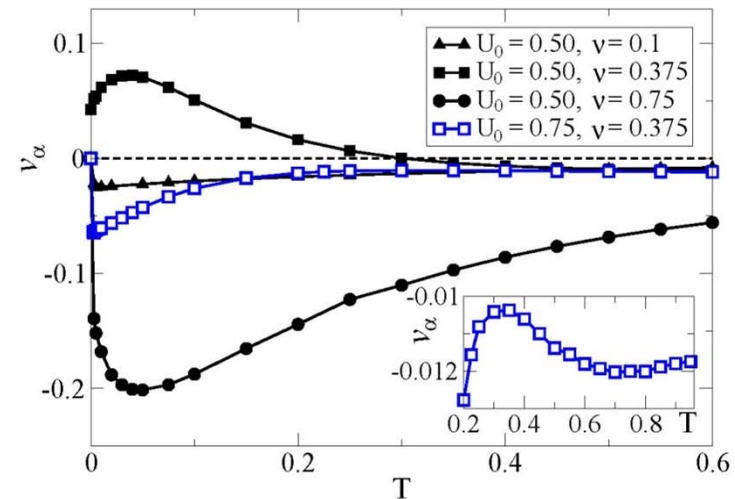
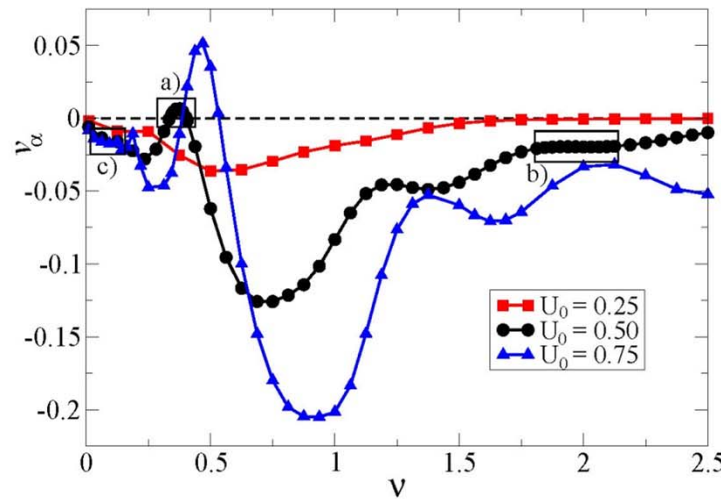
Earlier models: flashing subdiffusive ratchets

[V.Kharchenko, I.Goychuk, New J.Phys., V.14, 043042 (2012)]

Interpretation



Transport optimization



Rigid motor connection with cargo

[I.Goychuk, V.Kharchenko, R.Metzler, Plos One, V.9, e91700 (2014)]

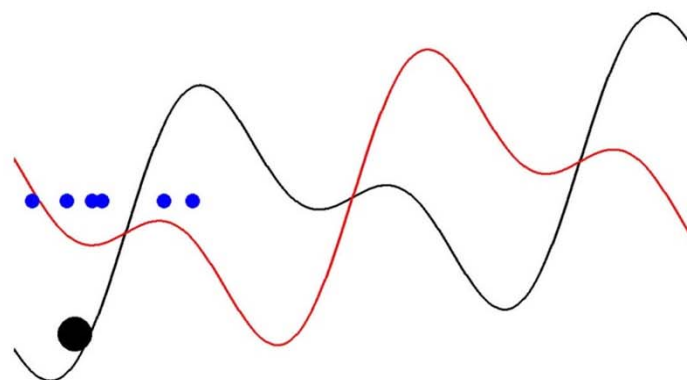
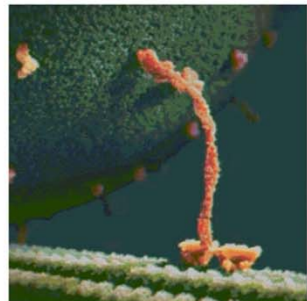
$$\begin{cases} \eta_0 \dot{x} = f(x, t) - \sum_{i=1}^N k_i(x - x_i) + \xi_0(t), & f(x, t) = -\frac{\partial V(x, t)}{\partial x} \\ \eta_i \dot{x}_i = k_i(x - x_i) + \sqrt{2\eta_i k_B T} \xi_i(t). \end{cases} \quad (8)$$

Viscous frictional constants: $\eta_i = k_i/v_i$

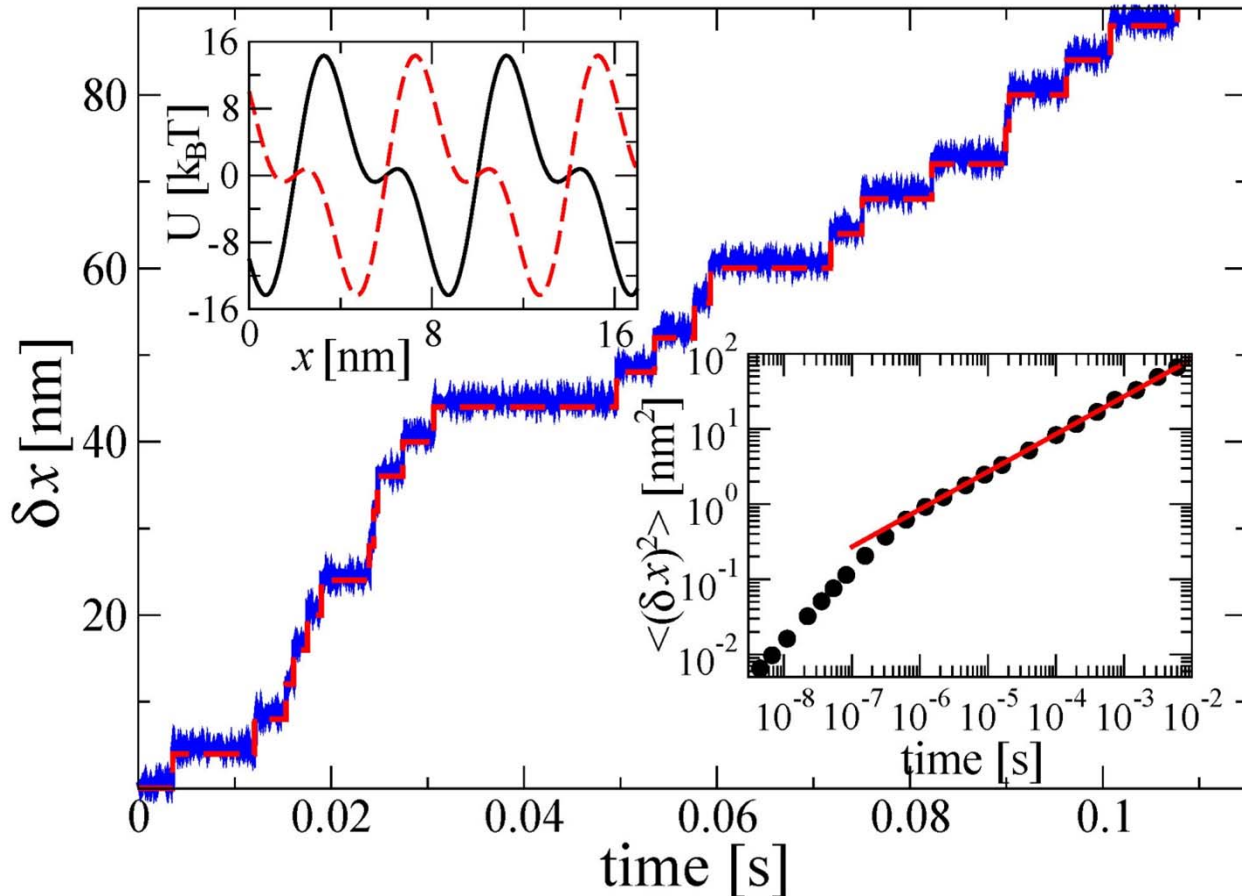
Driven potential: $V(x, t) = U(x) + f_0 x$

Periodic spatial potential: $U_{1,2}(x+L) = U_{1,2}(x)$, $U_1(x+L/2) = V_2(x)$

Used constants: $\alpha = 0.5$, $b = 10$, $C_{0.5} = 1.3$, $N = 12$

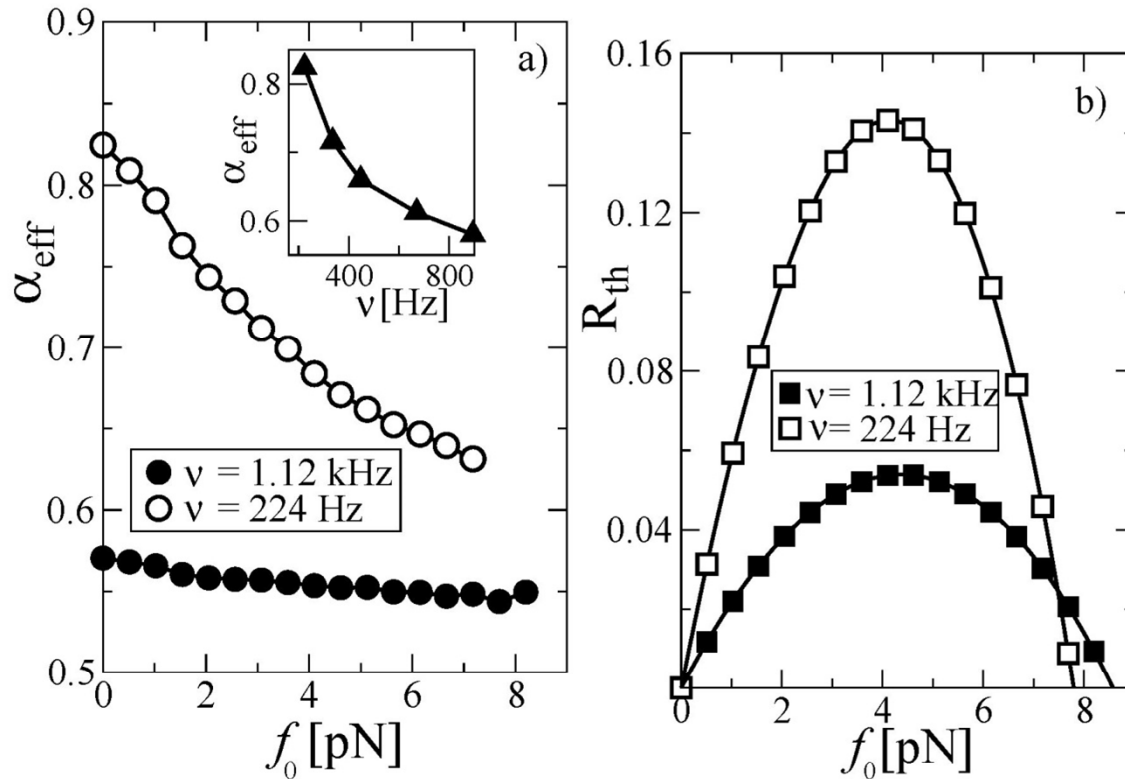


Normal transport and free subdiffusion



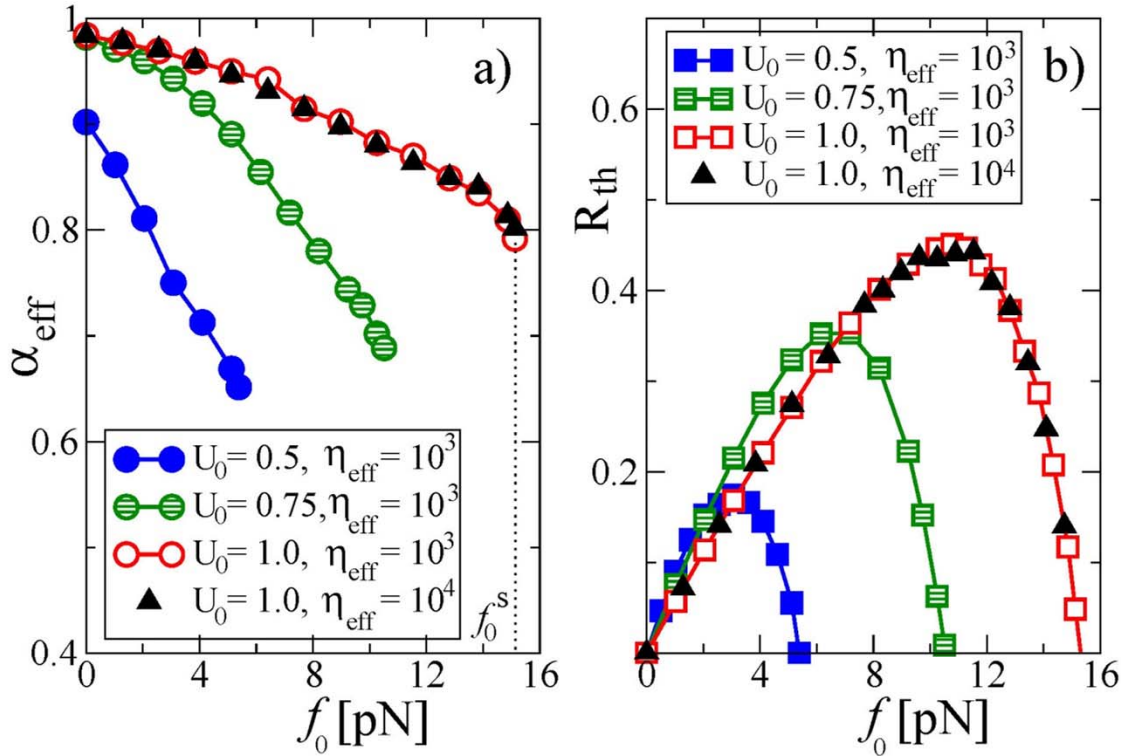
Single motor transport (full line) is almost perfectly locked to the potential fluctuations (broken red line depicting a renewal process counting the number of potential fluctuations in units of $L/2$) occurring with mean turnover frequency $v_{\text{turn}} = 112$ Hz, in a potential (top inset) with amplitudes $U_0 = 0.25$ eV ($U_0 = 1$ in dimensionless units) and $U_1 = 0.162$ eV ($\Delta V = 0.7$ eV), for $L = 8$ nm. A particle with an effective radius 300 nm (like a magnetic endosome) experiences asymptotically for $t \gg \tau_{\max} \approx 22.4$ sec an effective viscous friction enhanced by a factor of $\tilde{\eta}_{\text{eff}} = 10^4$ with respect to water. The bottom inset shows that on the relevant transient time scale the free particle subdiffuses with anomalous diffusion coefficient $D_\alpha \approx 368 \text{ nm}^2/\text{s}^{0.5}$.

Anomalous transport of large cargo particles



Anomalous transport of large cargo particles at lower potential amplitude, larger turnover rates, and in the presence of loading force f_0 . (a) Effective anomalous transport exponent α_{eff} and (b) thermodynamic efficiency R_{th} while working against a constant force f_0 near the end point of the simulations (0.224 sec or 10^6 in dimensionless units). The thermodynamic efficiency decays over time as $R_{\text{th}}(t) \propto 1/t^{1-\alpha_{\text{eff}}}$. The analysis considers the same particles, but here the potential height is reduced by factor of 2/3. Ensemble averaging is performed over 10^3 particles and random realizations of potential flashes. The inset in (a) shows the dependence of α_{eff} on the mean enzyme turnover frequency for $f_0 = 0$.

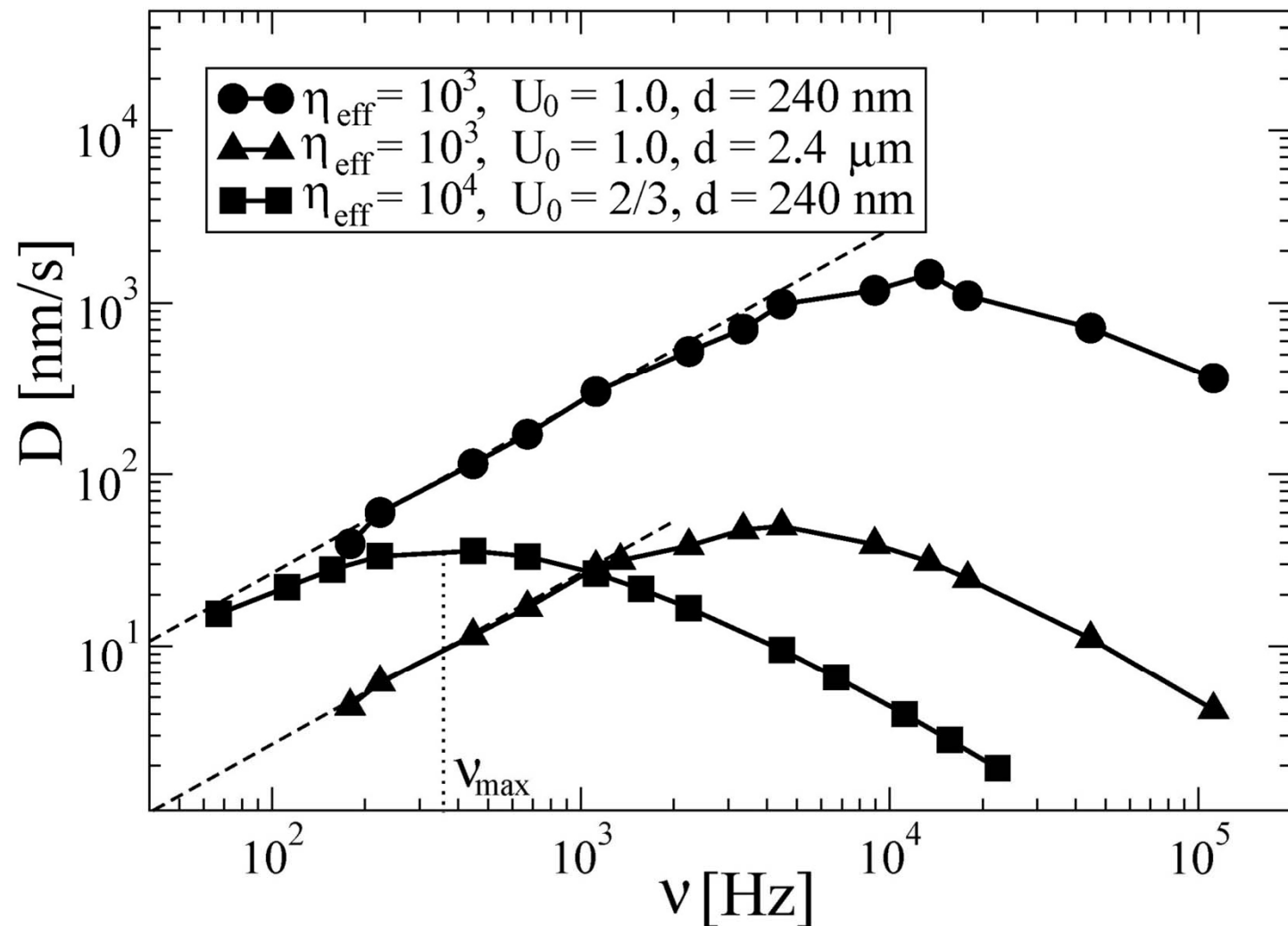
Anomalous transport of large cargo particles at $v_{\text{turn}} = 1.12 \text{ kHz}$



Dependence of (a) the effective transport exponent α_{eff} and (b) the thermodynamic efficiency R_{th} on the load f_0 , for three different potential amplitudes and for turnover frequency $v_{\text{turn}} = 1.12 \text{ kHz}$. Ensemble averaging is done over 10^3 particles and random realizations of potential flashes, $\tilde{\eta}_{\text{eff}} = 10^3$, $\tau_{\text{max}} = 22.4 \text{ sec}$, or $\tilde{\eta}_{\text{eff}} = 10^4$ and $\tau_{\text{max}} = 2240 \text{ sec}$. Matching of the results for two sets with the same amplitude $U_0 = 1.0$ indicates that $\eta\alpha$ is the characteristic quantity, rather than η_{eff} and τ_{max} separately. Efficiency is calculated at the end point of simulations 10^6 corresponding to $t = 0.224 \text{ sec}$.

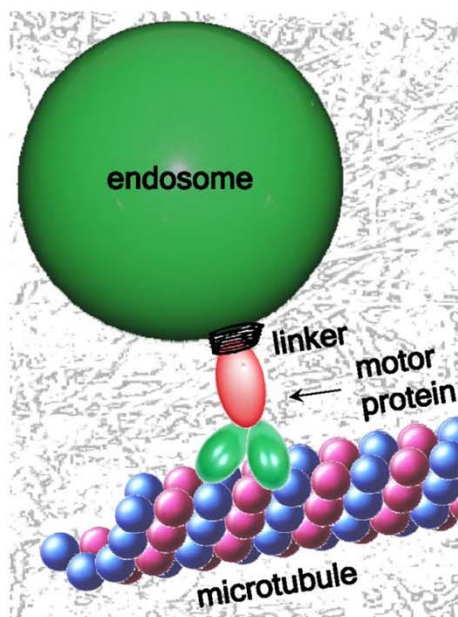
Delivery efficiency

In the ideal power-stroke regime $D_{\text{ideal}} = L^2 v_{\text{turn}} / d$



Elastic motor connection with cargo

[I.Goychuk, V.Kharchenko, R.Metzler, Phys.Chem.Chem.Phys., V.16, 16524 (2014)]

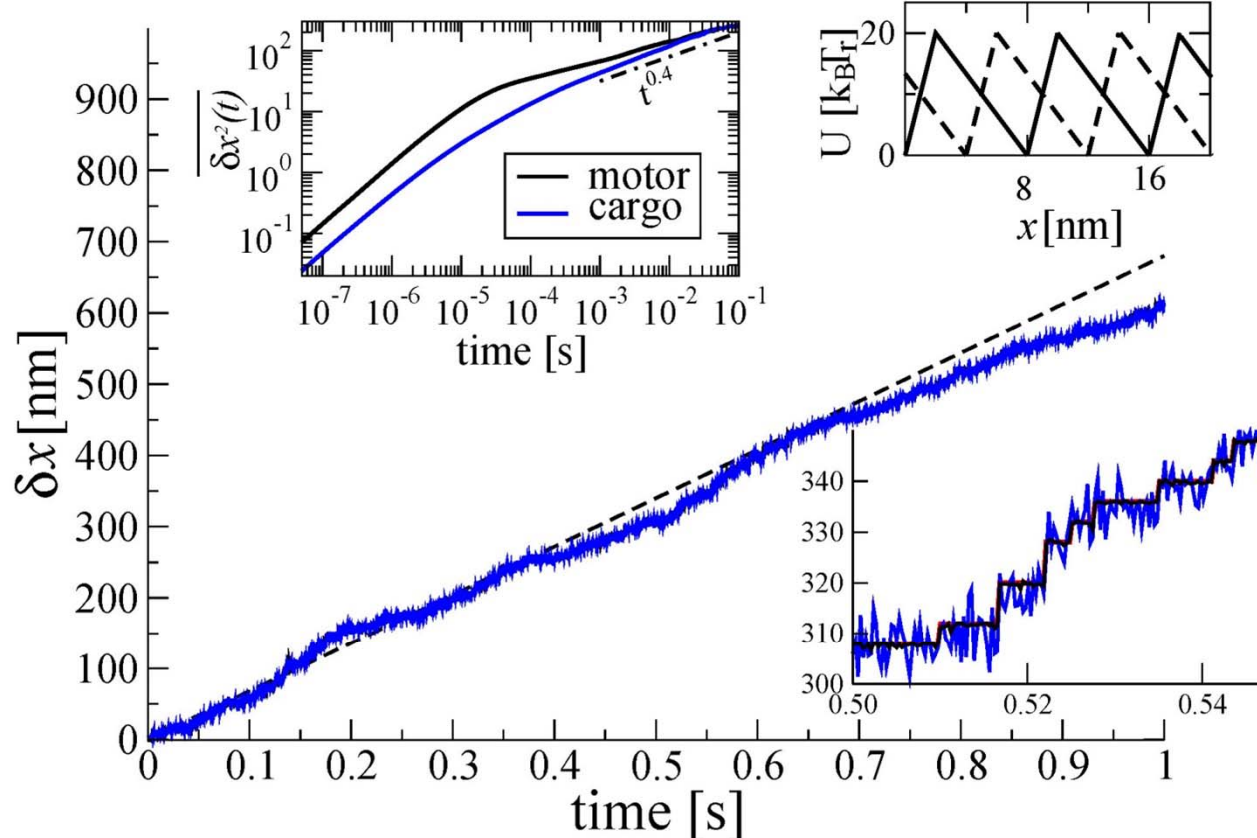


$$\left\{ \begin{array}{l} \eta_m \dot{x} = f(x, t) - k_L(x - y) + \sqrt{2\eta_m k_B T} \xi_m(t) \\ \eta_c \dot{y} = k_L(x - y) - \sum_{i=1}^N k_i(y - y_i) + \sqrt{2\eta_c k_B T} \xi_0(t) \\ \eta_i \dot{y}_i = k_i(x - x_i) + \sqrt{2\eta_i k_B T} \xi_i(t). \end{array} \right. \quad (9)$$

Set	η_{eff}	k_L [pN/nm]	v_{turn} [Hz]
S1	3×10^4	0.320	85
S2	3×10^3	0.320	85
S3	3×10^3	0.032	85
S4	3×10^4	0.032	85
S5	3×10^4	0.320	17
S6	3×10^4	0.032	17

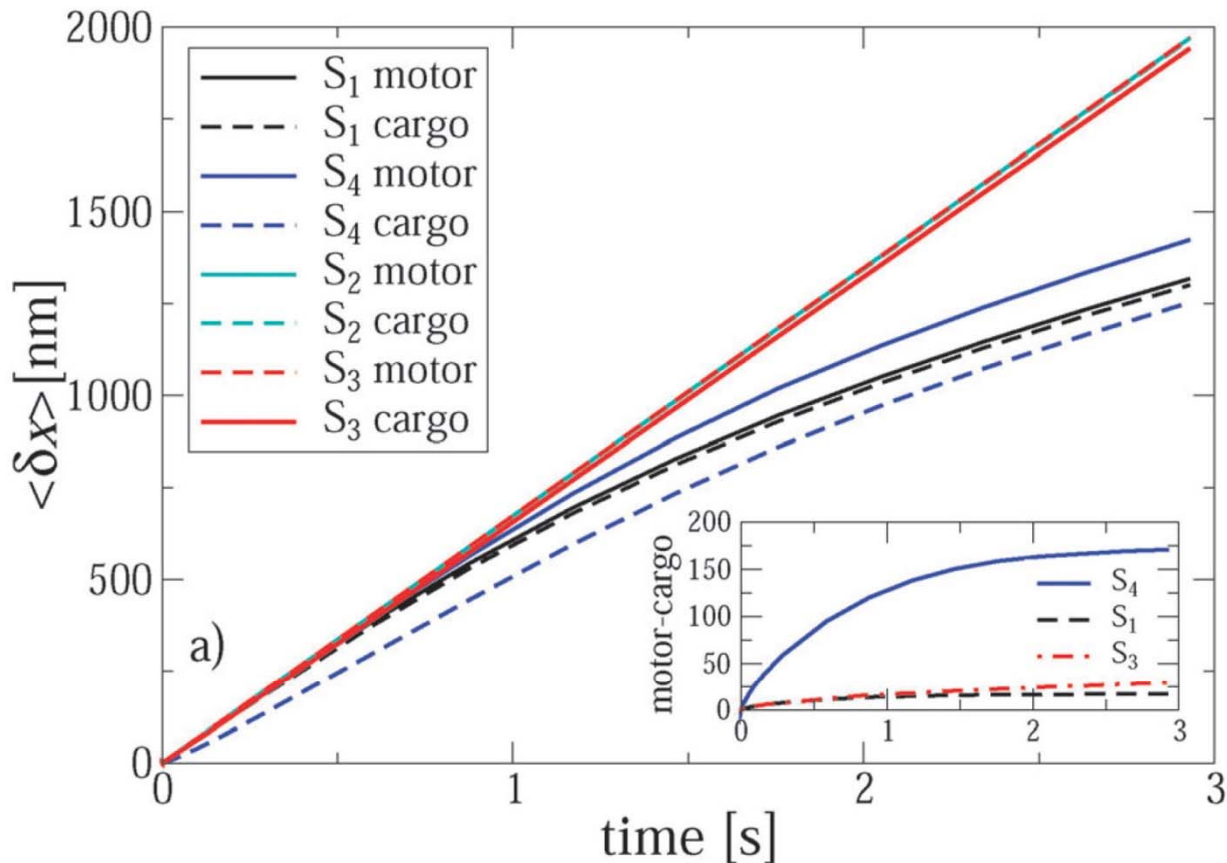
Subdiffusion and normal transport

$$v_{\text{turn}} = 85 \text{ Hz}, k_L = 0.32 \text{ pN/nm}, \eta_{\text{eff}} = 3 \cdot 10^3$$



Positions of motor (black line) and cargo (blue line) versus time for a single trajectory realization. The broken black lines depict the dependence of the averaged (over many trajectory realizations) position of motor on time in the case of a perfect synchronization (ideal power stroke like mechanism). Upper inset, shows diffusion of coupled motor and cargo in the absence of binding potential. The position variances have been obtained using a corresponding single-trajectory time averaging. The lower inset magnifies a part of motor and cargo trajectories making the step-wise motion of motor obvious. It is perfectly synchronized with the potential switches. Cargo randomly fluctuates around the motor position.

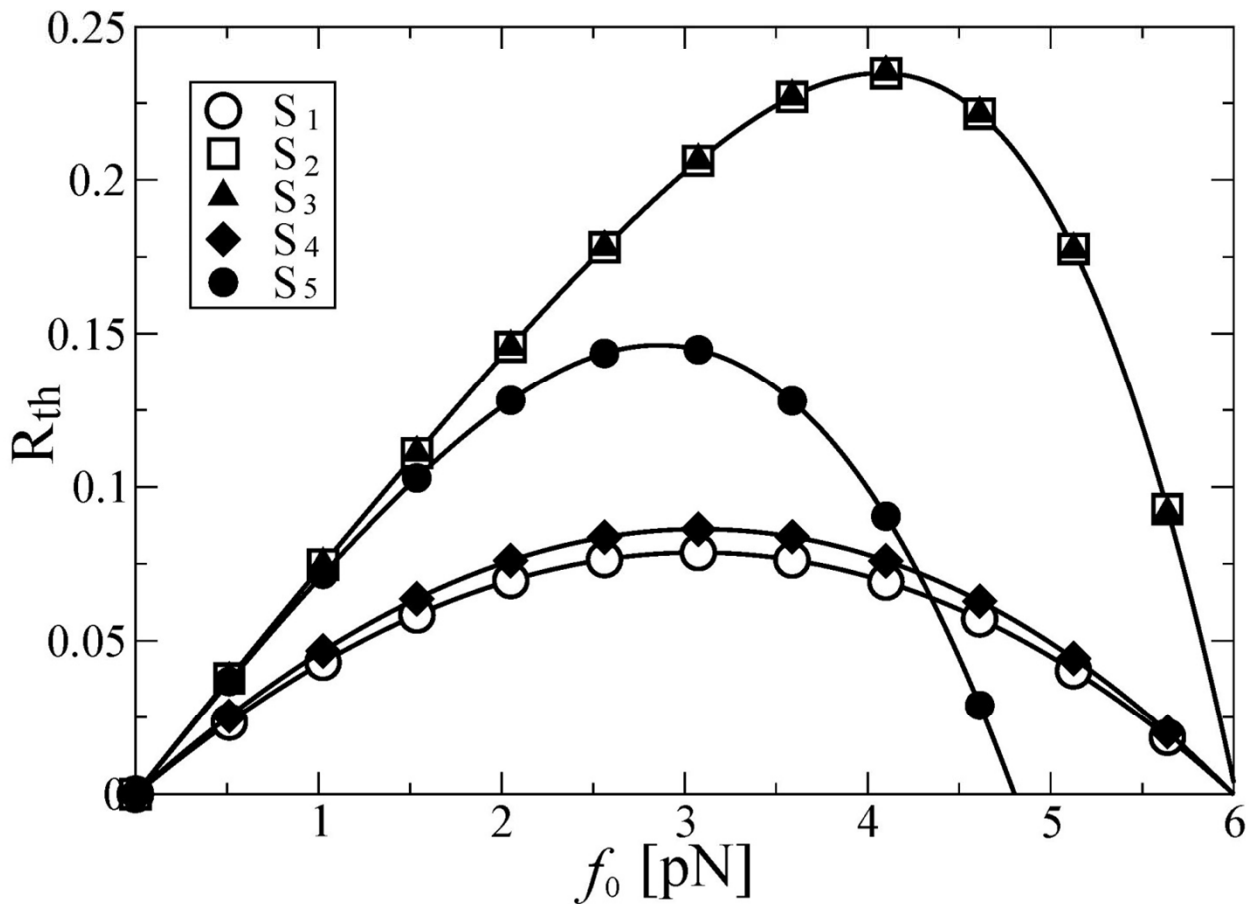
Motor-cargo distance for S1, S2, S4 and S4



Set	η_{eff}	k_L [pN/nm]	v_{turn} [Hz]
S1	3×10^4	0.320	85
S2	3×10^3	0.320	85
S3	3×10^3	0.032	85
S4	3×10^4	0.032	85

Ensemble-averaged trajectories (10^3 different realizations) of motor and cargo particles for different sets of parameters turnover frequency 85 Hz. Inset shows the differences between the motor and cargo positions for the chosen sets. Transport of smaller particles is normal. (a) Within the anomalous transport regime of larger particles, the motor-cargo distance increases and saturates at about 17 nm for S1 and about 170 nm for S4. This means that weaker linker can be unfolded during the transport of larger particle, or even break down.

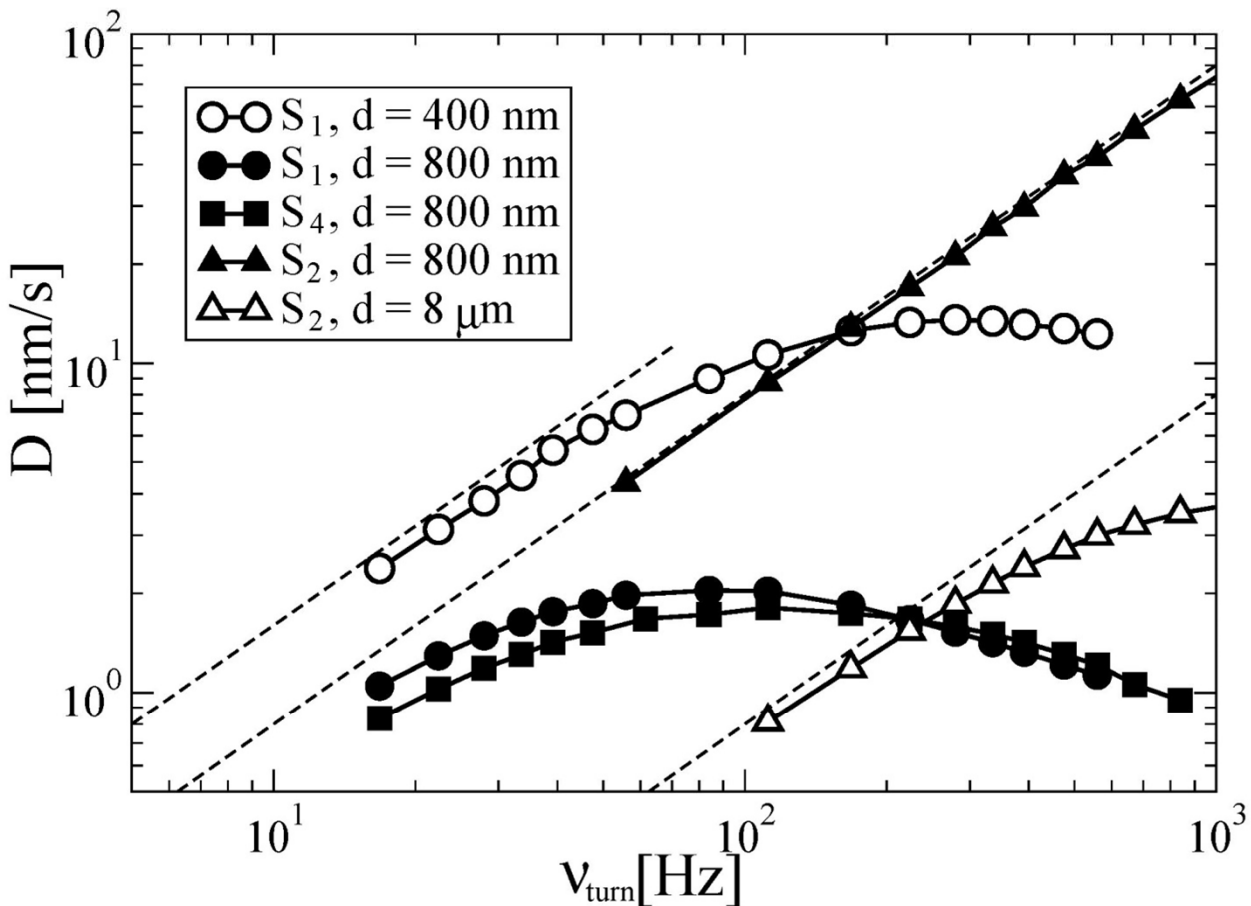
Thermodynamic efficiency



Set	η_{eff}	k_L [pN/nm]	v_{turn} [Hz]
S1	3×10^4	0.320	85
S2	3×10^3	0.320	85
S3	3×10^3	0.032	85
S4	3×10^4	0.032	85
S5	3×10^4	0.320	17

Thermodynamic efficiency as function of loading force f_0 at the end of simulations (corresponding to $t_{max} = 2.94$ s) for different sets.

Transport delivery efficiency



Set	η_{eff}	k_L [pN/nm]	v_{turn} [Hz]
S1	3×10^4	0.320	85
S2	3×10^3	0.320	85
S3	3×10^3	0.032	85
S4	3×10^4	0.032	85
S5	3×10^4	0.320	17

Transport delivery efficiency D as function of turnover frequency v_{turn} for different sets of parameters and different delivery distances d . Broken lines correspond to ideal power-stroke dependence $D_{\text{ideal}} = L^2 v_{\text{turn}} / d$, to compare with.